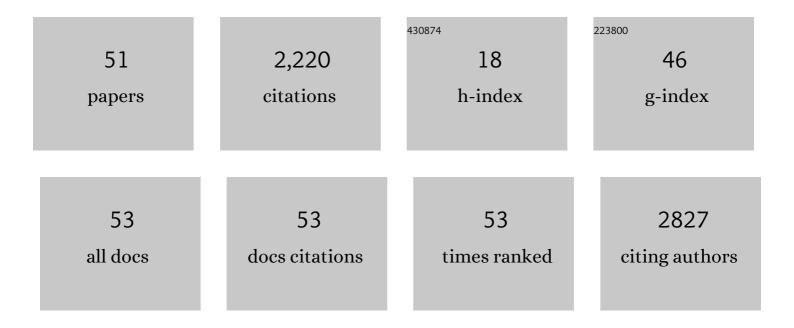
Anton O Oliynyk

List of Publications by Year in descending order

Source: https://exaly.com/author-pdf/7531531/publications.pdf Version: 2024-02-01



#	Article	IF	CITATIONS
1	Trends in Bulk Compressibility of Mo _{2–<i>x</i>} W _{<i>x</i>} BC Solid Solutions. Chemistry of Materials, 2022, 34, 2569-2575.	6.7	0
2	Tie-Dyeing with Foraged Acorns and Rust: A Workshop Connecting Green Chemistry and Environmental Science. Journal of Chemical Education, 2022, 99, 2431-2437.	2.3	4
3	Finding the Next Superhard Material through Ensemble Learning. Advanced Materials, 2021, 33, e2005112.	21.0	33
4	Machine Learning: Finding the Next Superhard Material through Ensemble Learning (Adv. Mater.) Tj ETQq0 0 0 rgI	3T /Overlo 21.0	ck 10 Tf 50
5	Three Rh-rich ternary germanides in the Ce–Rhâ^'Ge system. Journal of Solid State Chemistry, 2021, 304, 122585.	2.9	2
6	Ternary Rare-Earth-Metal Nickel Indides RE ₂₃ Ni ₇ In ₄ (RE = Gd, Tb,) Tj ETQq 60, 17900-17910.	0 0 0 rgB1 4.0	[/Overlock] 2
7	Significant Variability in the Photocatalytic Activity of Natural Titanium-Containing Minerals: Implications for Understanding and Predicting Atmospheric Mineral Dust Photochemistry. Environmental Science & Technology, 2020, 54, 13509-13516.	10.0	17
8	Coloured intermetallic compounds LiCu2Al and LiCu2Ga. Journal of Solid State Chemistry, 2020, 292, 121703.	2.9	4
9	Half-Heusler Structures with Full-Heusler Counterparts: Machine-Learning Predictions and Experimental Validation. Crystal Growth and Design, 2020, 20, 6469-6477.	3.0	20
10	Machine Learning for Materials Scientists: An Introductory Guide toward Best Practices. Chemistry of Materials, 2020, 32, 4954-4965.	6.7	224
11	Tailorable Indirect to Direct Band-Gap Double Perovskites with Bright White-Light Emission: Decoding Chemical Structure Using Solid-State NMR. Journal of the American Chemical Society, 2020, 142, 10780-10793.	13.7	58
12	A Tale of Seemingly "Identical―Silicon Quantum Dot Families: Structural Insight into Silicon Quantum Dot Photoluminescence. Chemistry of Materials, 2020, 32, 6838-6846.	6.7	22
13	Dehydrocoupling – an alternative approach to functionalizing germanium nanoparticle surfaces. Nanoscale, 2020, 12, 6271-6278.	5.6	2
14	Machine Learning in Materials Discovery: Confirmed Predictions and Their Underlying Approaches. Annual Review of Materials Research, 2020, 50, 49-69.	9.3	75
15	Atomic Substitution to Balance Hardness, Ductility, and Sustainability in Molybdenum Tungsten Borocarbide. Chemistry of Materials, 2019, 31, 7696-7703.	6.7	11
16	Alkaline Earth Metal–Organic Frameworks with Tailorable Ion Release: A Path for Supporting Biomineralization. ACS Applied Materials & Interfaces, 2019, 11, 32739-32745.	8.0	30
17	Single-Crystal Automated Refinement (SCAR): A Data-Driven Method for Determining Inorganic Structures. Inorganic Chemistry, 2019, 58, 9004-9015.	4.0	9
18	Solving the Coloring Problem in Half-Heusler Structures: Machine-Learning Predictions and Experimental Validation. Inorganic Chemistry, 2019, 58, 9280-9289.	4.0	17

IF

CITATIONS

19	Virtual Issue on Machine-Learning Discoveries in Materials Science. Chemistry of Materials, 2019, 31, 8243-8247.	6.7	23
20	Lattice strain and texture analysis of superhard Mo _{0.9} W _{1.1} BC and ReWC _{0.8} <i>via</i> diamond anvil cell deformation. Journal of Materials Chemistry A, 2019, 7, 24012-24018.	10.3	2
21	Quaternary rare-earth sulfides RE3M0.5M′S7 (M = Zn, Cd; M′ = Si, Ge). Journal of Solid State Chemistry, 2019, 278, 120914.	2.9	8
22	Synthesis, structure, and properties of rare-earth germanium sulfide iodides RE3Ge2S8I (RE = La, Ce,) Tj ETQq0 C) 0 rgBT /C 2:9)verlock 10 Tf
23	Production of Atmospheric Organosulfates via Mineral-Mediated Photochemistry. ACS Earth and Space Chemistry, 2019, 3, 424-431.	2.7	10
24	Silicon Nanoparticles: Are They Crystalline from the Core to the Surface?. Chemistry of Materials, 2019, 31, 678-688.	6.7	49
25	Hexagonal Double Perovskite Cs ₂ AgCrCl ₆ . Zeitschrift Fur Anorganische Und Allgemeine Chemie, 2019, 645, 323-328.	1.2	16
26	Discovery of Intermetallic Compounds from Traditional to Machine-Learning Approaches. Accounts of Chemical Research, 2018, 51, 59-68.	15.6	94
27	Enhancement in surface mobility and quantum transport of Bi2â^'xSbxTe3â^'ySey topological insulator by controlling the crystal growth conditions. Scientific Reports, 2018, 8, 17290.	3.3	17
28	Not Just Par for the Course: 73 Quaternary Germanides RE4M2XGe4 (RE = La–Nd, Sm, Gd–Tm, Lu; M =) Tj E Chemistry, 2018, 57, 14249-14259.	TQq0 0 0 4.0	rgBT /Overloc 9
28 29			0
	Chemistry, 2018, 57, 14249-14259. Identifying an efficient, thermally robust inorganic phosphor host via machine learning. Nature	4.0	9
29	Chemistry, 2018, 57, 14249-14259. Identifying an efficient, thermally robust inorganic phosphor host via machine learning. Nature Communications, 2018, 9, 4377. Machine Learning Directed Search for Ultraincompressible, Superhard Materials. Journal of the	4.0	9 228
29 30	Chemistry, 2018, 57, 14249-14259. Identifying an efficient, thermally robust inorganic phosphor host via machine learning. Nature Communications, 2018, 9, 4377. Machine Learning Directed Search for Ultraincompressible, Superhard Materials. Journal of the American Chemical Society, 2018, 140, 9844-9853. How To Optimize Materials and Devices <i>via</i>	4.0 12.8 13.7	9 228 215
29 30 31	Chemistry, 2018, 57, 14249-14259. Identifying an efficient, thermally robust inorganic phosphor host via machine learning. Nature Communications, 2018, 9, 4377. Machine Learning Directed Search for Ultraincompressible, Superhard Materials. Journal of the American Chemical Society, 2018, 140, 9844-9853. How To Optimize Materials and Devices <i>via</i> Design of Experiments and Machine Learning: Demonstration Using Organic Photovoltaics. ACS Nano, 2018, 12, 7434-7444. Polyanionic Gold–Tin Bonding and Crystal Structure Preference in	4.0 12.8 13.7 14.6	9 228 215 219
29 30 31 32	Chemistry, 2018, 57, 14249-14259. Identifying an efficient, thermally robust inorganic phosphor host via machine learning. Nature Communications, 2018, 9, 4377. Machine Learning Directed Search for Ultraincompressible, Superhard Materials. Journal of the American Chemical Society, 2018, 140, 9844-9853. How To Optimize Materials and Devices <i>>via</i> Design of Experiments and Machine Learning: Demonstration Using Organic Photovoltaics. ACS Nano, 2018, 12, 7434-7444. Polyanionic Gold–Tin Bonding and Crystal Structure Preference in REAu _{1.5} Sn _{O.5} (RE = La, Ce, Pr, Nd). Inorganic Chemistry, 2018, 57, 10736-10743. Complex Crystal Chemistry of Yb ₆ SoSo So </td <td>4.0 12.8 13.7 14.6 4.0</td> <td>9 228 215 219 4</td>	4.0 12.8 13.7 14.6 4.0	9 228 215 219 4
29 30 31 32 33	Chemistry, 2018, 57, 14249-14259. Identifying an efficient, thermally robust inorganic phosphor host via machine learning. Nature Communications, 2018, 9, 4377. Machine Learning Directed Search for Ultraincompressible, Superhard Materials. Journal of the American Chemical Society, 2018, 140, 9844-9853. How To Optimize Materials and Devices <i>via</i> Design of Experiments and Machine Learning: Demonstration Using Organic Photovoltaics. ACS Nano, 2018, 12, 7434-7444. Polyanionic Gold–Tin Bonding and Crystal Structure Preference in REAu _{1.5} Sn _{0.5} (RE = La, Ce, Pr, Nd). Inorganic Chemistry, 2018, 57, 10736-10743. Complex Crystal Chemistry of Yb ₆ (CuCa) ₅₀ and Yb ₆ (CuCa) Sorven at Different Synthetic Conditions. Crystal Growth and Design, 2018, 18, 6091-6099. Searching for Missing Binary Equiatomic Phases: Complex Crystal Chemistry in the Hfâ~'In System.	4.0 12.8 13.7 14.6 4.0 3.0	9 228 215 219 4 5

ARTICLE

#

ANTON O OLIYNYK

#	Article	IF	CITATIONS
37	Classifying Crystal Structures of Binary Compounds AB through Cluster Resolution Feature Selection and Support Vector Machine Analysis. Chemistry of Materials, 2016, 28, 6672-6681.	6.7	76
38	High-Throughput Machine-Learning-Driven Synthesis of Full-Heusler Compounds. Chemistry of Materials, 2016, 28, 7324-7331.	6.7	256
39	Gd ₁₂ Co _{5.3} Bi and Gd ₁₂ Co ₅ Bi, Crystalline Doppelgäger with Low Thermal Conductivities. Inorganic Chemistry, 2016, 55, 6625-6633.	4.0	18
40	Data mining our way to the next generation of thermoelectrics. Scripta Materialia, 2016, 111, 10-15.	5.2	106
41	Many Metals Make the Cut: Quaternary Rare-Earth Germanides RE4M2InGe4(M = Fe, Co, Ni, Ru, Rh, Ir) and RE4RhInGe4Derived from Excision of Slabs in RE2InGe2. Inorganic Chemistry, 2015, 54, 2780-2792.	4.0	8
42	The phase equilibria and crystal structure of the phases in the Hf–Ti–P system. Journal of Alloys and Compounds, 2015, 633, 75-82.	5.5	1
43	Investigation of phase equilibria in the quaternary Ce–Mn–In–Ge system and isothermal sections of the boundary ternary systems at 800 ŰC. Journal of Alloys and Compounds, 2015, 622, 837-841.	5.5	6
44	Ternary rare-earth manganese germanides RE3Mn2Ge3 (RE=Ce–Nd) and a possible oxygen-interstitial derivative Nd4Mn2Ge5OO.6. Journal of Alloys and Compounds, 2014, 602, 130-134.	5.5	4
45	Rare-earth transition-metal gallium chalcogenides RE3MGaCh7 (M=Fe, Co, Ni; Ch=S, Se). Journal of Solid State Chemistry, 2014, 210, 79-88.	2.9	24
46	Quaternary Germanides RE4Mn2InGe4(RE = La–Nd, Sm, Gd–Tm, Lu). Inorganic Chemistry, 2013, 52, 8264-8271.	4.0	13
47	Phase Equilibria in the Mo–Fe–P System at 800 °C and Structure of Ternary Phosphide (Mo _{1–<i>x</i>} Fe _{<i>x</i>}) ₃ P (0.10 ≤i>x ≤0.15). Inorganic Chemistry, 2013, 52, 983-991.	4.0	17
48	Rare-earth manganese germanides RE2+MnGe2+ (RE=La, Ce) built from four-membered rings and stellae quadrangulae of Mn-centred tetrahedra. Journal of Solid State Chemistry, 2013, 206, 60-65.	2.9	7
49	Ternary rare-earth ruthenium and iridium germanides RE3M2Ge3 (RE=Y, Gd–Tm, Lu; M=Ru, Ir). Journal of Solid State Chemistry, 2013, 202, 241-249.	2.9	10
50	The Ti-Fe-P system: phase equilibria and crystal structure of phases. Open Chemistry, 2013, 11, 1518-1526.	1.9	9
F1	Green Chemistry Applied to Transition Metal Chalcogenides through Synthesis, Design of Experiments,		

Life Cycle Assessment, and Machine Learning. , 0, , .